High-order harmonic generation by excited helium: The atomic polarization effect

Vitali Averbukh*
Department of Chemistry, Technion—Israel Institute of Technology, Haifa 32000, Israel
(Received 5 November 2003; published 20 April 2004)

Atomic polarization can have a profound effect on the generation of the high-order harmonics during the interaction of the polarized atom with intense field. In this work, the atomic polarization effect is investigated for the specific case of the $2\,^1P$ helium subject to infrared radiation. The strong coupling between the $2\,^1P$ and $2\,^1S$ states of helium is taken into account using a multichannel version of the strong-field approximation of Lewenstein and co-workers [Lewenstein *et al.*, Phys. Rev. A **49**, 2117 (1994); Antoine *et al.*, *ibid.* **53**, 1725 (1996)]. The analysis reveals a strong dependence of the high-order harmonic generation efficiency on the atomic polarization. While the occurrence of the predicted effect can be explained in terms of the recollision model, its magnitude is deeply affected by the fast population oscillations between the excited bound states. Moreover, the induced bound-bound transitions bring about the interesting double-maximum structure in the ellipticity dependences of the emitted harmonics, both maxima occurring for nonzero field ellipticities. This unusual structure shows up even for the high-energy harmonics generated solely by the bound-continuum mechanism.

DOI: 10.1103/PhysRevA.69.043406 PACS number(s): 42.50.Hz, 42.65.Ky, 32.80.Wr

I. INTRODUCTION

The dependence of the high-order harmonic generation (HHG) by rare gas atoms on the polarization of the incident radiation has been studied both experimentally and theoretically (see, e.g., Refs. [1–4]). It has been found that the high-order harmonics become strongly suppressed with increasing ellipticity of the laser beam. This phenomenon has found its explanation within the framework of the recollision model of the atomic HHG [5,6]. Classically speaking, the electron leaving an atom under the influence of elliptically polarized field acquires a nonzero drift velocity which precludes its efficient rescattering from the atomic core. In this situation, the chances for the electron's recombination back to the atomic ground state accompanied by the HHG become increasingly small as one departs further from the zero-field ellipticity. In fact, the observed damping of the high-order harmonics in elliptically polarized field has been considered as a principal experimental evidence for the validity of the recollision mechanism of HHG.

While the effect of the *electromagnetic wave polarization* on the atomic HHG is understood, the possible influence of the *atomic polarization* on the process has not been considered so far. In the present work we show that, in fact, the effect of the atomic polarization on the spectrum of the generated high-order harmonics can be no less significant than the one of the incident field polarization. It turns out that the harmonic intensities can depend strongly on the spatial orientation of the atomic angular momentum with respect to the polarization of the incident laser field. Let us elucidate the role of the atomic polarization in the strong-field dynamics by considering the interaction of a two-electron atom being initially in a $(n+1)^1P[ns^1(n+1)p^1]$ excited state with linearly polarized field. In this case, the atomic p orbital occupied by the "active" outer electron of the system can be oriented, for example, along the electric-field axis or in the perpendicular plane. In the case of the parallel orientation of the atomic orbital and the ionizing field, the well-known three-step scenario of the atomic HHG [5,6] can take place. The ionized electron can be driven back by the oscillating field to recombine to a bound state generating the high-frequency radiation. However, in the case of the perpendicular orientation of the p orbital with respect to the electric field, no ionization along the field polarization direction is possible due to the symmetry of the atomic orbital. For example, if an electron occupying a p_y orbital interacts with the field polarized along the x axis, it cannot undergo a transition to the scattering state $\Phi_{\vec{p}}^{(-)}$ with zero asymptotic momentum in the y direction:

$$\langle \Phi_{\vec{p}}^{(-)}(r^2,\vec{p}\cdot\vec{r})|eE_x x|\Phi_{p_y}(r^2,y)\rangle = 0 \quad \text{if } p_y = 0. \qquad (1)$$

In this perpendicular configuration, the ionized electron must attain some nonzero velocity along the symmetry axis of the p orbital. The electron drifts away from the atomic core reducing the probability of the recollision event and with it also the high-order harmonic intensities. Thus, the atomic polarization can have a profound effect on the HHG spectrum, at least in the low-frequency, high-intensity regime where the recollision model is valid.

The nonzero drift velocity of the electron being ionized in the perpendicular configuration can also lead to unusual ellipticity dependences of the emitted high-order harmonics. Indeed, within the recollision picture, the reason for the damping of the HHG at nonzero ellipticity is the drift of the electron induced by the elliptically polarized field. But if the electron was initially bound in a p orbital oriented perpendicularly to the main axis of the ellipse, there can be an interplay between the symmetry- and field-induced drifts.

*Present address: Theoretische Chemie, Physikalisch-Chemisches Institut, Universität Heidelberg, In Neuenheimer Feld 229, D-69120 Heidelberg, Germany.

Eventually one can find that the high-order harmonics possess maximal intensities at some nonzero field ellipticity. Such an "anomalous" ellipticity dependence has been found in HHG by the ground-state atoms for the harmonics with energies within the range of the atomic ionization potential (i.e., for the low-order and the threshold harmonics) [3,7,8]. However, the "anomalous" ellipticity dependence for the harmonics of arbitrarily high order is expected to be a distinctive feature of the polarized atom setup. In what follows we shall explore these atomic and field polarization effects in some detail considering the interaction of the excited helium atom with infrared (IR) radiation.

II. MULTICHANNEL STRONG-FIELD APPROXIMATION FOR THE HHG SPECTRUM OF EXCITED HELIUM

Regard a helium atom prepared in a superposition of the ground state and the second excited singlet state

$$\Phi_0 = \alpha\Phi_{1\,^1S} + \beta e^{i\varphi}\Phi_{2\,^1P}, \quad \alpha^2 + \beta^2 = 1. \tag{2}$$

The polarization of the atom, i.e., the spatial orientation of the p orbital of $\Phi_{2\,^1P}$, is defined by the polarization of the excitation pulse used for the preparation of the state Φ_0. The effect of the atomic polarization on the HHG can be understood by comparing the spectra of the excited helium atoms interacting with the electric field polarized along the symmetry axis of the p orbital (i.e., as the excitation pulse) with HHG resulting from the interaction with the perpendicularly polarized field.

The $2\,^1P$ state of helium has the binding energy of about 3.37 eV, only a bit lower than those of ground-state alkali atoms. Since alkali metal vapors interacting with IR radiation are known to generate high-order harmonics [9], we shall concentrate on the interaction of the excited helium with an IR source of intensity up to 10^{-3} a.u. Just as in the case of the alkali, the HHG by the excited helium can be affected by the bound-state dynamics. In particular, one should take into account the transition from the $2\,^1P$ state to the first excited singlet state, $2\,^1S$, characterized by the relatively small ($\approx$0.6 eV) energy splitting and large ($\approx$2.9 a.u.) transition dipole moment. This transition is allowed in the case where the IR pulse is polarized as the excitation pulse, but is forbidden in the case of perpendicularly polarized fields. The other possible bound-bound transitions, e.g., $2\,^1P-1\,^1S$ and $2\,^1P-3\,^1S$, characterized by much larger energy differences and significantly smaller transition dipole moments, can be neglected in the first approximation. These considerations allow one to approximate the time-dependent wave function of the helium atom interacting with IR field as

$$\Psi(t) \approx a_{1\,^1S}(t)\Phi_{1\,^1S} + a_{2\,^1S}(t)\Phi_{2\,^1S} + a_{2\,^1P}(t)\Phi_{2\,^1P} + \int_{-\infty}^{\infty}\frac{d^3p}{(2\pi\hbar)^3}b(\vec{p},t)\Phi_{\vec{p}}^{(-)}, \tag{3}$$

where $\Phi_{\vec{p}}^{(-)}$ are the scattering states corresponding to the single ionization of helium.

A series of further approximations will provide a simple semianalytical solution for the bound and continuum state amplitudes in Eq. (3). First of all, let us assume the single active electron approximation. In the studied case, it is justified by the very significant energy separation between the two helium orbitals occupied initially. The relevant bound states of helium [see Eq. (3)] will be represented using single-electron hydrogenic orbitals with such effective charges that the corresponding $\langle r^2\rangle$ expectation values match the realistic ones, $Z_{\mathrm{eff}}(1\,^1S)=1.5855$, $Z_{\mathrm{eff}}(2\,^1S)=1.6158$, $Z_{\mathrm{eff}}(2\,^1P)=1.3797$. The crudity of this approximation can be estimated by calculating the $2\,^1P-2\,^1S$ transition dipole moment using the hydrogenic wave functions. It turns out that the matrix element is recovered with about 10% inaccuracy.

Regarding the bound-state coefficients [see Eq. (3)], one notes that the $1\,^1S$ state population should not be affected appreciably by the IR pulse. Indeed, the electric field is far too weak for tunneling ionization of the ground state and its frequency is too small to make any possible multiphoton transition efficient. Thus, one can assume

$$a_{1\,^1S}(t) = \alpha\,\exp(-iE_{1\,^1S}t/\hbar), \tag{4}$$

where $E_{1\,^1S}$ is the ground-state energy (we neglect the small ac Stark shift of the ground state). On the other hand, the excited $2\,^1S$ and $2\,^1P$ states are expected to be strongly coupled between themselves and appreciably coupled to the continuum. Let us calculate the continuum state amplitudes using the strong-field approximation of Lewenstein and coworkers [10,4]. Within this approach, the continuum states are represented by plane waves and their population is assumed to be insignificant comparing to the bound-state population. The resulting expression for the continuum state amplitudes reads

$$b(\vec{p},t) = \frac{i}{\hbar}\int_0^t \sum_{j=2\,^1S,\,2\,^1P} e\vec{E}(t')\cdot\vec{d}_j \times[\vec{p}+(e/c)\vec{A}(t)-(e/c)\vec{A}(t')]a_j(t') \times\exp\left\{-\frac{i}{\hbar}\int_{t'}^{t}\frac{[\vec{p}+(e/c)\vec{A}(t)-(e/c)\vec{A}(t'')]^2}{2m}dt''\right\}dt', \tag{5}$$

where $\vec{E}(t)$ and $\vec{A}(t)$ are the electric field and the vector potential of the incident pulse, respectively, and $\vec{d}_j$ are the matrix elements for the transitions from the excited states to the plane wave continuum states:

$$\vec{d}_j(\vec{p}) = \langle\exp(i\vec{p}\cdot\vec{r}/\hbar)|\vec{r}|\Phi_j\rangle, \quad j = 2\,^1S, 2\,^1P. \tag{6}$$

Contrary to the single-bound-state expressions of Refs. [10,4], Eq. (5) describes ionization from a pair of strongly coupled bound states. Using the assumption of the low continuum population, one can calculate the excited-state amplitudes, a_j, within the two-state model. For linearly polarized field, the corresponding coupled equations read

$$i\hbar\dot{a}_{2\,^1S}(t) = E_{2\,^1S}\,a_{2\,^1S}(t) - e\vec{E}(t)\cdot\vec{d}_{2\,^1S-2\,^1P}\,a_{2\,^1P}(t),$$

$$i\hbar\,\dot{a}_{2\,^1P}(t) = E_{2\,^1P}\,a_{2\,^1P}(t) - e\vec{E}(t)\cdot\vec{d}^{*}_{2\,^1S-2\,^1P}\,a_{2\,^1S}(t), \quad (7)$$

where $\vec{d}_{2\,^1S-2\,^1P}=\langle\Phi_{2\,^1S}|\vec{r}\,|\Phi_{2\,^1S}\rangle$ is the matrix element for the $2\,^1P-2\,^1S$ transition and the excited-state coefficients should be normalized according to $|a_{2\,^1S}|^2+|a_{2\,^1P}|^2=\beta^2$ [see Eq. (2)]. The orientation of the $\vec{d}_{2\,^1S-2\,^1P}$ vector defines the spatial orientation of the $2p$ orbital. Let us introduce the angle θ between the symmetry axis of the $2p$ orbital and the field polarization axis: $\vec{E}\cdot\vec{d}_{2\,^1S-2\,^1P}=Ed_{2\,^1S-2\,^1P}\cos(\theta)$. For θ small enough, the dynamics of the $2\,^1P-2\,^1S$ transition in the IR field can be characterized by high-interaction-energy variation, $2eEd_{2\,^1S-2\,^1P}\cos(\theta)\gg E_{2\,^1P}-E_{2\,^1S}$. As shown by Ivanov and Corkum, under these conditions, the system (7) can be solved perturbatively [11]. The zeroth-order solution which neglects the energy splitting between the two atomic states reads

$$a^{(0)}_{2\,^1S}(t) = i\beta e^{i\varphi}\exp(-i\overline{E}t/\hbar) \times\sin\left[e\int_0^t E(t')d_{2\,^1S-2\,^1P}\cos(\theta)dt'/\hbar\right],$$

$$a^{(0)}_{2\,^1P}(t) = \beta e^{i\varphi}\exp(-i\overline{E}t/\hbar) \times\cos\left[e\int_0^t E(t')d_{2\,^1S-2\,^1P}\cos(\theta)dt'/\hbar\right], \quad (8)$$

where $\overline{E}=(E_{2\,^1P}+E_{2\,^1S})/2$. One can see that within the zeroth-order approximation, the ac Stark shifts of the excited states bring about their exact degeneracy. Since the high-interaction-energy requirement cannot be satisfied by a finite pulse during its switching on and switching off, the validity of the above solution in the case of the interaction with laser pulses is limited by the additional condition [11]: $\hbar\omega \gg E_{2\,^1P}-E_{2\,^1S}$, where ω is the field frequency. In the opposite extreme case of small interaction energy, e.g., for $|\theta-\pi/2| \ll 1$, the excited-state coefficients attain the following simple form:

$$a_{2\,^1S}(t)\approx 0, \quad a_{2\,^1P}(t)\approx\beta e^{i\varphi}\exp(-iE_{2\,^1P}t/\hbar), \quad (9)$$

where the first equality is exact for $\theta=\pi/2$.

Equations (3)–(5), (8), and (9) define the approximate time-dependent wave function $\Psi(t)$ of the excited helium atom interacting with IR pulse. This wave function can be used in order to calculate the resulting HHG spectrum $I(\Omega)$ as the spectrum of the acceleration of the induced dipole moment $\vec{\mu}(t)$:

$$I(\Omega)=\Omega^4\left|\frac{1}{T}\int_0^T e^{-i\Omega t}\vec{\mu}(t)dt\right|^2, \quad \vec{\mu}(t)=\langle\Psi(t)|\vec{r}\,|\Psi(t)\rangle, \quad (10)$$

where T is the pulse duration. Substituting the wave function (3) and (5) into the expression for $\vec{\mu}(t)$, one obtains

$$\vec{\mu}(t) = 2e\,\mathrm{Re}\Bigg\{a^{*}_{2\,^1S}(t)a_{2\,^1P}(t)\vec{d}_{2\,^1S-2\,^1P} + a^{*}_{1\,^1S}(t)a_{2\,^1P}(t)\vec{d}_{1\,^1S-2\,^1P} + \sum_j\sum_k\frac{i}{\hbar} \times\int_0^t dt'\int_{-\infty}^{\infty}\frac{d^3P}{(2\pi\hbar)^3}e\vec{E}(t')\cdot\vec{d}_j[\vec{P}-(e/c)\vec{A}(t')]a_j(t') \times\exp\left[-\frac{i}{\hbar}\int_{t'}^t\frac{[\vec{P}-(e/c)\vec{A}(t'')]^2}{2m}dt''\right] \times\vec{d}^{*}_k[\vec{P}-(e/c)\vec{A}(t)]a^{*}_k(t)\Bigg\},$$

$$j=2\,^1S,\,2\,^1P, \quad k=1\,^1S,\,2\,^1S,\,2\,^1P. \quad (11)$$

The resulting expression is a generalization of the original result of Lewenstein and co-workers [10,4] to the case of several populated bound states. Within this multichannel version of the strong-field approximation, each harmonic amplitude is described as a sum of the bound-bound [the first two terms on the right-hand side (rhs) of Eq. (11)] and bound-continuum [the third term on the right-hand side (rhs) of Eq. (11)] contributions. Furthermore, the bound-continuum part is a coherent superposition of the amplitudes which are related to the various ionization-recombination paths characterized by different initial and final bound states.

III. THE EFFECT OF THE ATOMIC POLARIZATION ON THE HHG OF THE EXCITED HELIUM

The general features of the HHG spectrum of the excited helium atom can be predicted by considering the various terms contributing to the induced dipole moment (11). Let us consider first the HHG by the atom with the $2p$ orbital oriented parallel to the field polarization axis ($\theta=0$). In this "parallel" configuration, the first term on the rhs of the Eq. (11) arises from the transitions between the closely lying $2\,^1S$ and $2\,^1P$ states which are strongly coupled by the IR field. These transitions lead to the HHG plateau of the length equal to the maximal variation of the interaction energy [11]:

$$n^{b-b}_{\mathrm{cutoff}}=2eEd_{2\,^1S-2\,^1P}/(\hbar\omega). \quad (12)$$

For the fields considered in this work, this plateau is expected to be quite short, e.g., $n_{\mathrm{cutoff}}\approx 7$ either for the 1.6 μm field of the 32 TW/cm^2 intensity or for the 3.6 μm field of the 8 TW/cm^2 intensity.

It is interesting to note that although no $1\,^1S-2\,^1P$ transition occurs in our model, the coupling between these states gives rise to a nonlinear contribution to the induced dipole moment [the second term on the rhs of Eq. (11)]. At zero external field, a linear combination of the $2\,^1P$ and the $1\,^1S$ states is characterized by the time-dependent dipole, $\mu \sim\cos[(E_{2\,^1P}-E_{1\,^1S})t/\hbar]$. When the field is switched on, the population of the $2\,^1P$ state varies in time due to the $2\,^1S-2\,^1P$ coupling [see Eqs. (7) and (8)]. As a result, the second term on the rhs of Eq. (11) is expected to give rise to

a band of lines situated around the $1\,^1S-2\,^1P$ transition frequency. The number of the lines in this band is determined by the dynamics of the $2\,^1P-2\,^1S$ transition and should be about n^{b-b}_{cutoff} [see Eq. (12)].

The bound-continuum contribution to the induced dipole moment of the helium atom [the third term on the rhs of Eq. (11)] consists of the individual contributions of the transitions from the $2\,^1S$ or $2\,^1P$ state to the continuum and the recombinations to the $1\,^1S$, $2\,^1S$ or $2\,^1P$ state. The resulting HHG spectrum is qualitatively similar to the one of the excited $2s$ He^+ ion considered in Refs. [12,13]. The recombination back to one of the ionized states ($2\,^1S$ or $2\,^1P$) should give rise to the familiar HHG plateau with the cutoff at [5,6,10]:

$$n^{b-c}_{\text{cutoff}} \approx (-\bar{E} + 3.2U_p)/(\hbar\omega), \tag{13}$$

where U_p is the ponderomotive energy of a free electron in the field, $U_p = e^2E^2/(4m\omega^2)$. The recombination to the ground state leads to the increase of the emitted photon energy by about $\bar{E} - E_{1\,^1S}$. As a result, the second rescattering plateau of the same length [see Eq. (13)] is formed starting at the energy of $\bar{E} - E_{1\,^1S}$. It should be noted that the higher-energy plateau consists of lines shifted from the exact harmonic frequencies by $(\bar{E} - E_{1\,^1S}) \bmod \hbar\omega$. These lines become exact odd harmonics if the resonance condition ($\bar{E} - E_{1\,^1S} = N\hbar\omega$, N is odd) is satisfied [12]. The relative intensities of the two HHG plateaus are defined by the matrix elements for the recombination to the respective final states: $d^*_{2\,^1P,\,2\,^1S}(\vec{p})$ for the lower-energy plateau and $d^*_{1\,^1S}(\vec{p})$ for the higher-energy plateau (note that the effective charges used in the present work to mimic helium orbitals distort the two plateaus intensity ratio with respect to the Coulombic case considered in Ref. [13]). The two rescattering plateaus overlap if the ponderomotive energy is high enough, i.e., for $U_p > (2\bar{E} - E_{1\,^1S})/3.17 \approx 0.2$ a.u.

Since we are dealing with atoms being initially prepared in a superposition of the ground and the excited states, the initial amplitudes and phases of the superposition can affect the resulting HHG spectrum. Clearly, there should be a sufficient initial population of the $2\,^1P$ state in order for the HHG to be significant at all. On the other hand, only a substantial initial population of the ground state can reveal the double-plateau structure of the spectrum at $\theta \neq \pi/2$. Those contributions to the induced dipole moment (11) which correspond to the ionization from one of the excited states and the recombination to the ground state are affected also by the initial phase of the excited state coefficient, φ [see Eq. (2)]. Thus, the phases of the lines belonging to the higher-energy plateau are φ dependent (this feature is probably of relevance for the macroscopic response of the sample of the initially excited atoms). On the other hand, the contributions to $\vec{\mu}(t)$ responsible for the formation of the lower-energy plateau are φ independent. As will be shown below, it is the lower-energy plateau which is the common feature of the HHG spectrum at both parallel and perpendicular configurations

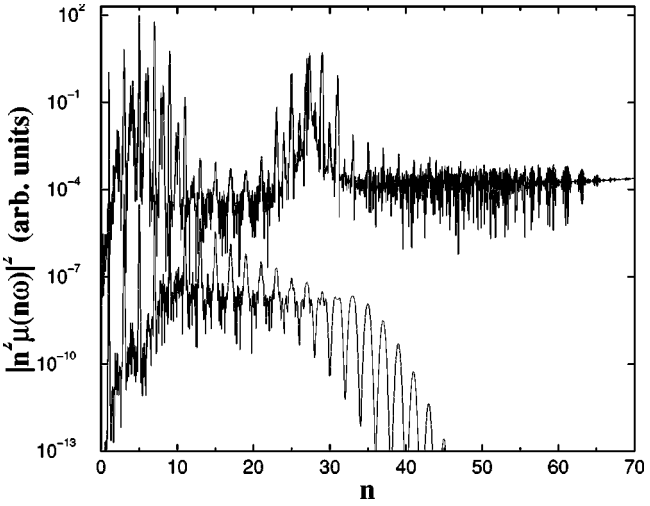

FIG. 1. The HHG spectra of helium atom prepared initially in a superposition of $1\,^1S$ and $2\,^1P$ states ($\alpha = \beta = 1/\sqrt{2}, \varphi = 0$). The incident field parameters are: $\omega = 0.028\,47$ a.u., $E_0 = 0.03$ a.u. Upper curve, the field is linearly polarized along the axis of the atomic p orbital; lower curve, the field is linearly polarized perpendicularly to the axis of the atomic p orbital.

and is thus of primary interest for this work. Consequently, in what follows we shall assume $\varphi = 0$.

In Fig. 1 we show the HHG spectra of the excited helium interacting with the 32-oscillation $\sin^2$ pulse of IR radiation of the frequency $\omega = 0.028\,47$ a.u. ($\bar{E} - E_{1\,^1S} = 27\hbar\omega$) and the peak field strength $E_0 = 0.03$ a.u. The field frequency used in the calculation is greater but not much greater than the $2\,^1S-2\,^1P$ energy splitting and the high-frequency requirement for the validity of the solution (8) in the case of a pulse is, strictly speaking, not satisfied. Consequently, we have used a numerical solution of Eq. (7) for the calculation of the HHG spectrum at the parallel configuration. It should be noted, nevertheless, that even at the frequency of 0.028 47 a.u., the Ivanov-Corkum solution leads to the harmonic intensities which are in a very good agreement with the results of the numerical solution. The reason for this is that the high-order harmonics are produced mainly after the pulse has been switched on, i.e., when the high-interaction-energy requirement is satisfied (see the discussion after Eq. (8) and Ref. [11]). One can see that the parallel configuration spectrum shown in Fig. 1 embodies all the features predicted by the qualitative analysis of the contributions to the induced atomic dipole moment (11). The two bound-continuum plateaus of the length of $-\bar{E} + 3.17U_p \approx 35\hbar\omega$ shifted from each other by the $27\hbar\omega$ energy difference appear in the spectrum along with the two bands of harmonics due to the transitions between the strongly coupled $2\,^1S$ and $2\,^1P$ states. The formation of the low-energy harmonic band due to the bound-bound transitions is reflected also in the field-intensity dependence of the high-order harmonics. As the field becomes stronger, the successive harmonics belonging to the rescattering plateau get enhanced to join the bound-bound plateau. The functional character of the enhancement is that of the Bessel function of large order and small argument [11], i.e., very roughly $I_n \sim \exp[-2n\,\sinh^{-1}(n/x)]$, where n is the har-

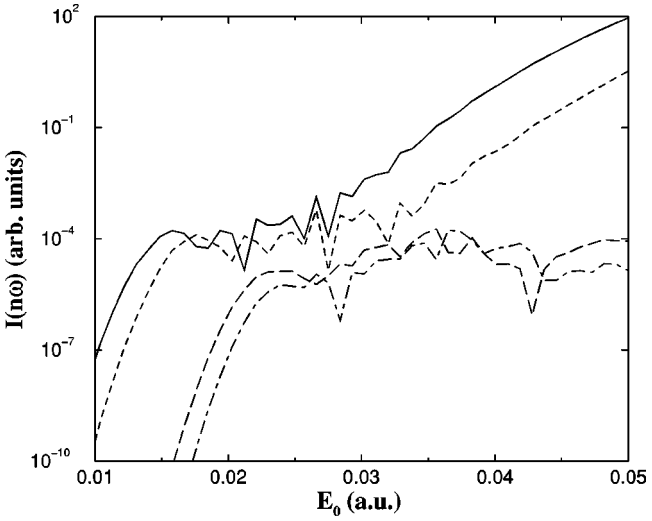

FIG. 2. Field strength dependence of the 13th (full line), 15th (dashed line), 23rd (long-dashed line), and 25th (dashed-dotted line) harmonics in the parallel configuration. Continuous wave field of the frequency $\omega=0.028\,47$ a.u. and zero ground-state population ($\alpha=0$, $\beta=1$) are assumed. The lower-order harmonics (13th and 15th) become strongly enhanced due to the $2\,^1S-2\,^1P$ oscillations, while the higher-order ones (23th and 25th) stay in the rescattering plateau.

monic order and the small argument x is proportional to the field strength. This steep rise of the harmonics is illustrated in Fig. 2. The predicted behavior of the band of the high-order harmonics in the excited helium is different from the one occurring in the alkalis [9,14,15], where the condition of the multiphoton resonance is required for the harmonic enhancement. The reason for the difference between the two systems is that the regime of the high interaction energy, $2eEd_{ns-np} \gg E_{np}-E_{ns}$, is not reached in the alkalis, in particular due to the relatively high energy differences between the strongly coupled *ns* and *np* states.

Turning now to the HHG in the perpendicular ($\theta=\pi/2$) configuration, we note that in this case the first two terms in the expression (11) for the induced dipole moment vanish by symmetry. Indeed, the electric field polarized perpendicularly to the p orbital symmetry axis cannot induce a transition to a s orbital. Consequently, the assumption (3) for the helium wave function made in this work is insufficient to describe the contribution of the bound-bound transitions to the HHG in perpendicular configuration. While a more detailed analysis than the one given here is needed to describe the actual role of the bound-bound transitions to the HHG in this case, their contribution is probably not going to be important for the high-order harmonics with energies exceeding the ionization energy of the $2\,^1P$ state. Symmetry considerations can be also used to show that in the perpendicular configuration there can be no recombination of the ionized electron into the ground $1\,^1S$ state. As a result, the bound-continuum contribution to the HHG at $\theta=\pi/2$ consists of a single plateau due to the ionization from and the recombination to the $2\,^1P$ state only (in other words, the $2\,^1P$ state plays the role of the effective ground state of the system). The angular distribution of the electron ionization from the p orbital oriented perpendicularly to the ionizing field is such that the probability for the electron emission along the field polarization axis is zero [see Eq. (1)]. Consequently, the ionized electron cannot be driven by the field back to the core which should lead to the damping of the recombination probability. Thus, the efficiency of the HHG process in the perpendicular ($\theta=\pi/2$) configuration should be significantly smaller than in the parallel ($\theta=0$) one. The dramatic effect of the atomic polarization on the HHG spectrum is demonstrated in Fig. 1. The comparison of the HHG spectra computed once for the parallel and another time for the perpendicular orientation of the atomic orbital with respect to the incident field shows that the HHG spectrum corresponding to the perpendicular configuration exhibits only a single (lower-energy) rescattering plateau. Moreover, the intensity of the lower-energy plateau in the perpendicular configuration is more than two orders of magnitude lower than in the parallel one. Thus, the atomic polarization effect is well pronounced.

The semianalytical approach exploited here allows one to obtain a crude order-of-magnitude estimate of the magnitude of the atomic polarization effect as a function of the parameters of the system. To this end, let us consider the case of nonoverlapping plateaus in the HHG spectrum of the parallel configuration, i.e., either $U_p<0.2$ a.u. or $\alpha \ll \beta$. Our calculations of the induced dipole moment (11) of the excited helium show that the ionization-recombination path giving the dominant contribution to the HHG spectrum at the parallel configuration is the one involving $2\,^1P$ state both as the initial and the final one. Let us thus simplify the problem by neglecting all other contributions. Furthermore, let us assume a cw field and substitute the $2\,^1P$ population by its optical cycle average: $\beta^2[1+J_0(2eE_0d_{2\,^1S-2\,^1P}/\hbar\omega)]/2$ and β^2 for the parallel and perpendicular configurations, respectively [see Eqs. (8) and (9)]. In this simplified picture, the expressions for the harmonic amplitudes in the parallel and in the perpendicular configurations are of the same type, namely,

$$\mu_{\parallel,\perp}(n\omega) \sim \int_0^{2\pi/\omega} dt\, e^{-in\omega t} \int_0^t dt' \int_{-\infty}^{\infty} \frac{d^3P}{(2\pi\hbar)^3} \times d_x^{x,y}[\vec{P}-(e/c)\vec{A}(t')]E_x(t') \times \exp\left\{-\frac{i}{\hbar}\int_{t'}^{t} \frac{[\vec{P}-(e/c)\vec{A}(t'')]^2}{2m}dt''\right\} \times \exp\left[\frac{iE_{2\,^1P}(t-t')}{\hbar}\right] d_x^{x,y*}[\vec{P}-(e/c)\vec{A}(t)], \tag{14}$$

where the field is polarized along the x axis and the d_x matrix elements [see Eq. (6)] with the superscripts x and y correspond to the p_x and p_y orbitals, i.e., to the parallel $[\mu_\parallel(n\omega)]$ and the perpendicular $[\mu_\perp(n\omega)]$ configurations respectively. The evaluation of the time and momentum integrals in Eq. (14) can be done by steepest descent methods [10]. As a result, the values of the integrals are related to the magnitudes of the integrands at the stationary phase values of the variables. One can use this property in order to estimate the $\mu_\parallel(n\omega)/\mu_\perp(n\omega)$ ratio for the highest-order harmonic (n_{cutoff})

in the low-energy rescattering plateau. More specifically, let us employ the stationary phase (imaginary) value of the initial kinematic momentum, $\vec{P}-(e/c)\vec{A}(t')$, and take the rest of the values of the integration variables from the kinematic model of the atomic HHG (see Ref. [16]). The resulting expression is

$$\left|\frac{\mu_{\parallel}(n_{\mathrm{cutoff}}\omega)}{\mu_{\perp}(n_{\mathrm{cutoff}}\omega)}\right|^2 \approx \left[1+J_0\left(\frac{2eE_0 d_{2\,^1S-2\,^1P}}{\hbar\omega}\right)\right]^2 \times\left[f_1\frac{E_0}{\omega^2}-\frac{f_2}{E_0}\right]^2, \tag{15}$$

where

$$f_1 \approx 0.895\frac{e}{\hbar}\sqrt{\frac{2|E_{2\,^1P}|}{m}}+4.48\times10^{-2}\frac{eZ_{\mathrm{eff}}^2(2\,^1P)\hbar}{a_0^2 m\sqrt{2m|E_{2\,^1P}|}} \approx 0.617 \text{ a.u.},$$
$$f_2 \approx 1.41\times10^{-3}\frac{Z_{\mathrm{eff}}^4(2\,^1P)\hbar^3}{ea_0^4 m\sqrt{2m|E_{2\,^1P}|}}+3.55\times10^{-2}\frac{Z^{\mathrm{eff}2}(2\,^1P)\hbar}{ea_0^2}\sqrt{\frac{2|E_{2\,^1P}|}{m}} \approx 4.39\times10^{-2} \text{ a.u.} \tag{16}$$

are the functions of the atomic parameters. Of course, Eq. (15) has a meaning only if $f_1E_0/\omega^2 > f_2/E_0$, a condition which is easily met in the parameter region considered in this work.

The leading term in the above harmonic intensity ratio scales as E_0^2/ω^4. Thus, the effect of the atomic polarization on the HHG spectrum is most prominent in the high-intensity, low-frequency regime, exactly where the Lewenstein-type theory used to describe the phenomenon is valid. In fact, the field-strength dependence of the estimated intensity ratio consists of the monotonous rise [the second factor on the rhs of Eq. (15)] due to the recollision process modulated by the oscillating function [the first factor on the rhs of Eq. (15)] resulting from the variation of the mean population of the $2\,^1P$ state. The field strength dependences of the atomic polarization effect calculated both using the Fourier transforms of the induced dipole moments (11) and the simple approximation (15) are shown in Fig. 3 for two values of the field frequency ($\omega=0.012\,67$ a.u. and $\omega=0.028\,47$ a.u.). As expected, the atomic polarization effect is much more pronounced for the lower frequency, but even in the higher-frequency case the effect is quite dramatic: the atomic polarization changes the HHG efficiency by two to four orders of magnitude. Figure 3 shows that the "exact" results are indeed represented by rising curves modulated by oscillations. The results of the steepest descent estimation lie almost entirely within an order of magnitude range from the "exact" ones. However, the simple approximation (15) misses both the period and the phase of the predicted oscillatory behavior. This means that the effect of the fast population oscillations between the strongly coupled bound states is a dynamical one and is not described well by the time-averaged $2\,^1P$ state population.

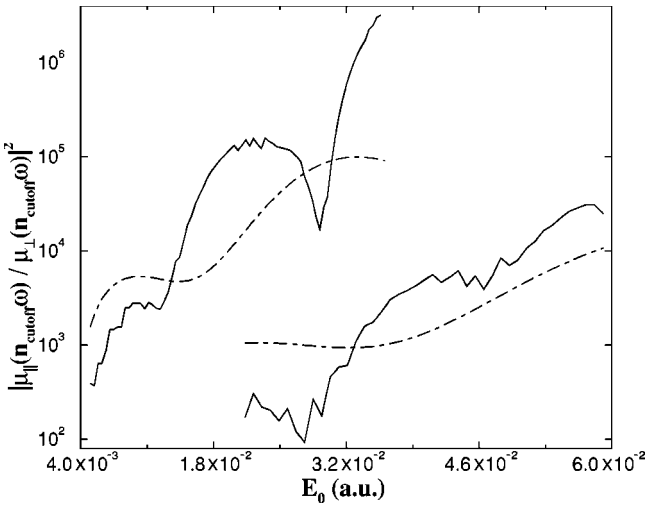

FIG. 3. The magnitude of the atomic polarization effect for the highest-order plateau harmonics as a function of the field strength. Zero ground-state population is assumed ($\alpha=0$, $\beta=1$). Higher pair of curves, $\omega=0.012\,67$ a.u. Lower pair of curves, $\omega=0.028\,47$ a.u., cw field is assumed in both cases. Full curves represent the Fourier transforms of the dipole moments calculated according to Eq. (11). The results are averaged over five successive harmonic orders, $n_{\mathrm{cutoff}}-6,\ldots,n_{\mathrm{cutoff}}+2$, to get rid of the erratic oscillations. Dashed-dotted curves represent the steepest descent estimation of Eq. (15).

To conclude the discussion of the atomic polarization effect, let us mention that the spatial orientation of the p orbital can continuously vary from parallel to the IR field polarization ($\theta=0$) to the perpendicular one ($\theta=\pi/2$). In the high-intensity, low-frequency case, where $|\mu_{\parallel}(n\omega)| \gg |\mu_{\perp}(n\omega)|$ (see Fig. 3), the deviation from the parallel configuration is accompanied by the uniform decrease of the harmonic intensities according to the $\cos^2(\theta)$ law up to the θ's at which $|\mu_{\parallel}(n\omega)|\cos(\theta) \leqslant |\mu_{\perp}(n\omega)|$.

IV. ELLIPTICITY DEPENDENCES OF THE HIGH-ORDER HARMONICS IN THE PERPENDICULAR CONFIGURATION

It has been demonstrated in Sec. III that HHG by the excited helium is suppressed when the atomic p orbital is oriented perpendicularly to the linearly polarized field. It is then natural to ask what should be the optimal field polarization for the HHG at the perpendicular configuration. As in the case of the atomic polarization dependence, the recollision model suggests a qualitative answer. In order to enhance the HHG, one has to compensate for the drift of the electron induced by the symmetry of the p orbital. This can be done using elliptically polarized field which is able itself to impart a drift momentum to the ionized electron. The compensation of the two effects can occur bringing about the most efficient HHG at some nonzero ellipticity. Since it is known that for symmetry reasons the atomic HHG is totally suppressed at circular polarization, the ellipticity (ε) dependences of the high-order harmonics at the perpendicular configuration are expected to attain their maxima at some $0<\varepsilon_{\max}<1$. Some idea about the typical value of $\varepsilon_{\max}$ can be obtained on the

basis of the recent experiment of Bhardwaj *et al.* [18]. The authors studied the nonsequential double ionization of benzene occurring according to the recollision mechanism. Since the highest occupied molecular orbital (HOMO) of benzene possesses a nodal plane (as the atomic p orbital in our case), the optimal ellipticity for the double ionization was found to be nonzero: $\varepsilon_{\max} \approx 0.1$. It should be taken into account, however, that the experiment involved a sample of unaligned molecules whereas here we consider a polarized atom.

In order to provide a quantitative description for the ellipticity dependence of the HHG by the studied system, we would like to consider the interaction of the excited helium atom with the elliptically polarized cw field, $\vec{E} = E_0/\sqrt{1+\varepsilon^2}[\cos(\omega t), \varepsilon \sin(\omega t), 0]$. The field of this type can induce more bound-bound transitions than the linearly polarized one. In our approximation it couples the ground and the three excited helium states: $1\,{}^1S$, $2\,{}^1S$, $2\,{}^1P_x$ and $2\,{}^1P_y$, i.e. two of the three degenerate p orbitals participate in the dynamics. The amplitudes of the bound states can be calculated by solving the corresponding four-level problem:

$$
\begin{aligned}
i\hbar \dot{a}_{1\,{}^1S}(t) &= E_{1\,{}^1S}\, a_{1\,{}^1S}(t) - e d_{1\,{}^1S-2\,{}^1P}[E_x(t) a_{2\,{}^1P_x}(t) \\
&\quad + E_y(t) a_{2\,{}^1P_y}(t)], \\
i\hbar \dot{a}_{2\,{}^1S}(t) &= E_{2\,{}^1S}\, a_{2\,{}^1S}(t) - e d_{2\,{}^1S-2\,{}^1P}[E_x(t) a_{2\,{}^1P_x}(t) \\
&\quad + E_y(t) a_{2\,{}^1P_y}(t)], \\
i\hbar \dot{a}_{2\,{}^1P_x}(t) &= E_{2\,{}^1P}\, a_{2\,{}^1P_x}(t) - e E_x(t)[d^*_{1\,{}^1S-2\,{}^1P}\, a_{1\,{}^1S}(t) \\
&\quad + d^*_{2\,{}^1S-2\,{}^1P}\, a_{2\,{}^1S}(t)], \\
i\hbar \dot{a}_{2\,{}^1P_y}(t) &= E_{2\,{}^1P}\, a_{2\,{}^1P_y}(t) - e E_y(t)[d^*_{1\,{}^1S-2\,{}^1P}\, a_{1\,{}^1S}(t) \\
&\quad + d^*_{2\,{}^1S-2\,{}^1P}\, a_{2\,{}^1S}(t)].
\end{aligned}
\tag{17}
$$

Since the ground state is only very weakly coupled to the excited states by the IR field, its population can be thought of as a constant [see Eq. (4)]. However, unlike at the linear field polarization, one cannot describe the transitions between the remaining three strongly coupled excited states by the Ivanov-Corkum perturbation theory, i.e., neglecting the $2\,{}^1S-2\,{}^1P$ splitting. The reason is that the matrices of the x and y components of the transition dipole moment in the three-state representation do not commute neither with one another nor with their commutator. It should be noted that exact solutions for a degenerate N level problem have been found in the case of circular polarization of the field (only under conditions of a special kind of a discrete symmetry) [19] and, more recently, in the general case for linear field polarization [20].

The exact solution of the system (17), can be found in the trivial case of $\varepsilon = 0$ for the $\Psi(t=0) = \Phi_{2\,{}^1P_y}$ initial condition, i.e., at the perpendicular configuration. In this case all the couplings vanish by symmetry and the $2\,{}^1P_y$ state behaves as a stationary one. It can also be regarded formally as a quasienergy (QE) state

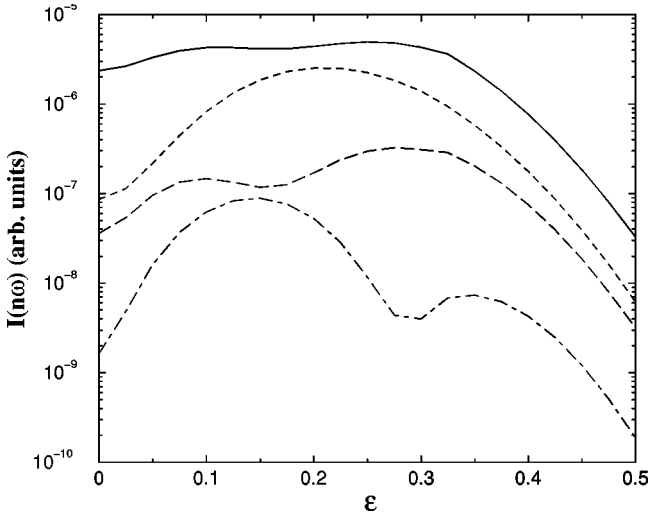

FIG. 4. Ellipticity dependences of the 15th (full line), 19th (dashed line), 21st (long-dashed line), and 27th (dashed-dotted line) harmonics. The electric field strength is $E_0 = 0.03$ a.u., the frequency is $\omega = 0.028\,47$ a.u. The harmonic curves are shifted along the intensity axis to afford a clear presentation.

$$
a_{2\,{}^1P_y}(t) = \exp\left(-i\frac{\lambda t}{\hbar}\right)\exp(-i n_0 \omega t), \tag{18}
$$

where $\lambda = \mathrm{mod}(E_{2\,{}^1P}, \hbar\omega)$ and $n_0\hbar\omega + \lambda = E_{2\,{}^1P}$. At nonzero ellipticity, the system (17) has to be solved numerically. The four QE solutions of Eq. (17),

$$
\begin{aligned}
a^{\alpha}_j(t) &= \exp\left(-i\frac{\lambda_\alpha t}{\hbar}\right)\sum_n a^{\alpha}_{j,n}\, \exp(in\omega t), \\
\alpha &= 1, \ldots, 4 \quad j = 1\,{}^1S,\, 2\,{}^1S,\, 2\,{}^1P_x, 2\,{}^1P_y,
\end{aligned}
\tag{19}
$$

were obtained numerically as functions of the field ellipticity. The correlation diagram for $\lambda_\alpha(\varepsilon)$, $0 \leqslant \varepsilon \leqslant 1$ was constructed and the QE state which correlates with $\Phi_{2\,{}^1P_y}$ at zero ellipticity was identified. The corresponding excited state amplitudes [see Eq. (19)] were substituted into the expression for the induced time-dependent dipole moment [Eq. (11) with $j = 2\,{}^1S,\, 2\,{}^1P_x, 2\,{}^1P_y$, $k = 1\,{}^1S,\, 2\,{}^1S,\, 2\,{}^1P_x,\, 2\,{}^1P_y$] to obtain the ellipticity dependent HHG spectrum of the excited helium. The resulting ellipticity dependences of the selected high-order harmonics are presented in Fig. 4. One can see that, as expected on the basis of the recollision arguments, all the harmonics attain their maximal intensities at nonzero field ellipticity. The calculations show that the average value for the $\varepsilon_{\max}$ is around 0.2 for the plateau harmonics, while for the cutoff harmonics a steady shift towards $\varepsilon_{\max} = 0.15$ is observed. The magnitude of the harmonic intensity enhancement at the optimal field ellipticity relatively to $\varepsilon = 0$ is typically around one order of magnitude (see Fig. 4), while for some harmonics it reaches more than two orders of magnitude.

The unexpected feature of the obtained results is the double-maximum structure of the ellipticity dependences of many of the high-order harmonics belonging to the rescatter-

ing plateau. This double-maximum character of the ellipticity dependence cannot be explained by the recollision model alone. In fact, the two maxima converge to a single one when the transitions from the $2\,^1P_y$ state to other bound states are artificially neglected. Consequently, the predicted unusual ellipticity dependence of the HHG is a result of the bound-bound dynamics. It has been verified that the bound-bound contribution to the intensities of the high-order harmonics presented in Fig. 4 is negligible. Thus, it is remarkable that the transitions between the bound states cause the double-maximum character of the ellipticity dependences of the harmonics belonging to the rescattering plateau.

V. CONCLUSIONS

In conclusion, it has been shown that the polarization of the atom can have a major effect on the structure and the intensity of the HHG spectrum. The atomic polarization effect has been described using the specific example of the $2\,^1P$ state of helium. The parallel orientation of the atomic p orbital relative to the electric field was found to be much more favorable for the HHG process than the perpendicular one. Depending on the incident field parameters, the harmonic intensity ratio between the two atomic polarizations can span the huge range 10^2-10^6, being the largest in the low-frequency, high-intensity regime. The nature of the very strong atomic polarization effect on the HHG spectrum can be understood qualitatively using recollision model and simple symmetry arguments. On the other hand, the character of the dependence of the effect on the incident field parameters cannot be explained by the recollision arguments alone. The reason is that the polarized atom dynamics is profoundly affected by the strong coupling between closely lying excited states. The fast oscillations between the excited states of helium cause an interesting oscillatory behavior of the magnitude of the atomic polarization effect, as quantified by the intensity ratio of the highest plateau harmonics in the "parallel" and the "perpendicular" configurations. They are also responsible for the strong nonresonant enhancement of the lower-order harmonics in the parallel (but not in the perpendicular) configuration. The bound-bound transitions were accounted for using the generalized version of the atomic HHG theory of Lewenstein and co-workers [10,4], which describes the ionization from and the recombination to a number of coupled bound states. This multichannel theory consistently takes into account both bound-bound and bound-continuum contributions to the HHG process. Moreover, it allows one to represent the bound-continuum contribution as a coherent superposition of the possible ionization-recombination paths characterized by different initial and final bound states. Retaining the intuitive structure of the original (single-bound-state) expressions, the more general theory helps to elucidate the unique role of the bound-bound transitions in the HHG by a polarized atom.

Another quantity reflecting the deep influence of the bound state dynamics on the HHG spectra of the excited helium is the ellipticity dependence of the high-order harmonics. The recollision picture combined with the symmetry arguments predicts that the plateau harmonics in the "perpendicular" configuration attain their maximal intensities at nonzero field ellipticity. The presented calculations show that this is indeed the case, however, the values of the optimal field ellipticity and the character of the ellipticity dependence are strongly affected by the bound-state oscillations. In particular, they bring about the double-maximum structure in the ellipticity dependences of many of the plateau harmonics. It should be noted that the unusual effect of the bound-state dynamics shows up for the harmonics corresponding to photon energies much exceeding the ionization potential of the initial bound state and being characterized by negligible bound-bound contribution to their intensities.

The interesting effects of the bound-bound transitions on the whole energy range of the HHG spectrum emitted by a polarized excited-state atom constitute the major qualitative difference between this system and the studied case of an aligned ground-state molecule [21,22]. The two systems can be indeed related by symmetry if both the valence atomic orbital and the HOMO possess a nodal plane. The effects of the molecular-orbital symmetry have been described without taking into account the field-induced transitions between the molecular bound states and the results were found to be consistent with the experimental ones [21,22]. Here we have shown that such a description would be fundamentally wrong in the case of a polarized excited-state atom. Consequently, the two symmetry-related systems appear to be quite different dynamically. This difference can be easily visualized if one considers, for example, the elliptically polarized field (see Sec. IV of the present work and Ref. [18]): the initial atomic polarization can be altered very fast by the incident beam, e.g., via $2\,^1P_y-2\,^1S-2\,^1P_x$ transition, whereas a change in the molecular orientation involves slow nuclear motion and occurs on much longer time scale.

The effects predicted in the present work have their origin in the interplay between the atomic orbital symmetry, bound-bound and rescattering dynamics. As such, they are not restricted to the HHG alone. Indeed, it is widely believed that the high-energy part of the atomic above-threshold ionization (ATI) spectrum is also formed by the rescattering mechanism (see Refs. [17,23,24] and references therein). Thus, it would be natural to suppose that the intensity of the ATI plateau of a polarized atom depends strongly on the spatial orientation of the atomic orbital (see Ref. [22] for the symmetry-related molecular problem). Moreover, the bound-bound transitions are expected to have a major influence on the atomic polarization dependence of the ATI. The exact character of this effect should be the subject of future investigations.

The presented calculations of the HHG by a polarized helium atom suggest that the atomic polarization effects are prominent enough to be observed experimentally. The recent experiments with ground- and excited-state alkalis [9] indicate feasibility of the experimental HHG studies in the regime similar to the one studied in the present work. As far as the target system is concerned, the $2\,^1P$ state of helium can be readily prepared by resonant excitation from the metastable $2\,^1S$ state [25]. A direct excitation from the ground state using a HHG source is also possible [26]. The polarization of the resulting state is related to that of the excitation beam and can be controlled as in the photoionization experiment of Johansson *et al.* [27]. The lifetime of the $2\,^1P$ he-

lium is about 0.57 ns [25–27] which is several orders of magnitude longer than the time needed for the interaction with the intense IR pulse. Consequently, the experimental observation of the effects proposed in the present work is feasible.

ACKNOWLEDGMENTS

This work was supported by the Basic Research Foundation administered by the Israeli Academy of Sciences and Humanities and by the Fund for the Promotion of Research at Technion. The author would like to thank Professor N. Moiseyev, Professor L. S. Cederbaum, Professor E. E. Nikitin, and Dr. M. Yu. Ivanov for fruitful discussions.

[1] K. S. Budil, P. Salières, A. L'Huillier, T. Ditmire, and M. D. Perry, Phys. Rev. A **48**, R3437 (1993).
[2] P. Dietrich, N. H. Burnett, M. Yu. Ivanov, and P. B. Corkum, Phys. Rev. A **50**, R3585 (1994).
[3] N. H. Burnett, C. Kan, and P. B. Corkum, Phys. Rev. A **51**, R3418 (1995).
[4] P. Antoine, A. L'Huillier, M. Lewenstein, P. Salières, and B. Carré, Phys. Rev. A **53**, 1725 (1996).
[5] P. B. Corkum, Phys. Rev. Lett. **71**, 1994 (1993).
[6] K. Kulander, K. Schafer, and J. Krause, in *Super-Intense Laser-Atom Physics*, Vol. 316 of *NATO Advanced Study Institutes, Series B: Physics*, edited by B. Piraux, A. L'Huillier, and K. Rzażewski (Plenum Press, New York, 1993), p. 316.
[7] M. Yu. Ivanov, T. Brabec, and N. Burnett, Phys. Rev. A **54**, 742 (1995).
[8] M. Kakehata, H. Takada, H. Yumoto, and K. Miyazaki, Phys. Rev. A **55**, R861 (1997).
[9] B. Sheehy, J. D. D. Martin, L. F. DiMauro, P. Agostini, K. J. Schafer, M. B. Gaarde, and K. C. Kulander, Phys. Rev. Lett. **83**, 5270 (1999); B. Sheehy, T. O. Clatterbuck, C. Lyngå, J. D. D. Martin, D. W. Kim, L. F. DiMauro, M. B. Gaarde, K. J. Schafer, P. Agostini, and K. C. Kulander, Laser Phys. **11**, 226 (2001); T. O. Clatterbuck, C. Lyngå, P. Colosimo, J. D. D. Martin, B. Sheehy, L. F. DiMauro, P. Agostini, and K. C. Kulander, J. Mod. Opt. **50**, 441 (2003).
[10] M. Lewenstein, Ph. Balcou, M. Yu. Ivanov, A. L'Huillier, and P. B. Corkum, Phys. Rev. A **49**, 2117 (1994).
[11] M. Yu. Ivanov and P. B. Corkum, Phys. Rev. A **48**, 580 (1993).
[12] J. B. Watson, A. Sanpera, X. Chen, and K. Burnett, Phys. Rev. A **53**, R1962 (1996).
[13] A. Sanpera, J. B. Watson, M. Lewenstein, and K. Burnett, Phys. Rev. A **54**, 4320 (1996).
[14] X. Chu, Shih-I Chu, and C. Laughlin, Phys. Rev. A **64**, 013406 (2001).
[15] M. B. Gaarde, and K. J. Schafer, Phys. Rev. A **64**, 013820 (2001).
[16] W. Becker, S. Long, and J. K. McIver, Phys. Rev. A **50**, 1540 (1994).
[17] M. Lewenstein, K. C. Kulander, K. J. Schafer, and P. H. Bucksbaum, Phys. Rev. A **51**, 1495 (1995).
[18] V. R. Bhardwaj, D. M. Rayner, D. M. Villeneuve, and P. B. Corkum, Phys. Rev. Lett. **87**, 253003 (2001).
[19] V. Averbukh, O. E. Alon, and N. Moiseyev, Phys. Rev. A **64**, 033411 (2001).
[20] J. H. McGuire, Kh. Kh. Shakov, and Kh. Yu. Rakhimov, J. Phys. B **36**, 3145 (2003).
[21] J. Muth-Böhm, A. Becker, and F. H. M. Faisal, Phys. Rev. Lett. **85**, 2280 (2000).
[22] F. Grasbon, G. G. Paulus, S. L. Chin, H. Walther, J. Muth-Böhm, A. Becker, and F. H. M. Faisal, Phys. Rev. A **63**, 041402(R) (2001).
[23] G. G. Paulus, F. Zacher, H. Walther, A. Lohr, W. Becker, and M. Kleber, Phys. Rev. Lett. **80**, 484 (1998).
[24] D. B. Milošević and F. Ehlotzky, Phys. Rev. A **58**, 3124 (1998).
[25] W. L. Williams and E. S. Fry, Phys. Rev. Lett. **20**, 1335 (1968); E. S. Fry and W. L. Williams, Phys. Rev. **183**, 81 (1969).
[26] J. Larsson, E. Mevel, R. Zerne, A. L'Huillier, C.-G. Wahlström, and S. Svanberg, J. Phys. B **28**, L53 (1995); M. Gisselbrecht, D. Descamps, C. Lyngå, A. L'Huillier, C.-G. Wahlström, and M. Meyer, Phys. Rev. Lett. **82**, 4607 (1999).
[27] A. Johansson, M. K. Raarup, Z. S. Li, V. Lokhnygin, D. Descamps, C. Lyngå, E. Mevel, J. Larsson, C.-G. Wahlström, S. Aloise, M. Gisselbrecht, M. Meyer, and A. L'Huillier, Eur. Phys. J. D **22**, 3 (2003).